VIII International Conference on Fracture Mechanics of Concrete and Concrete Structures
FraMCoS-8
J.G.M. Van Mier, G. Ruiz, C. Andrade, R.C. Yu and X.X. Zhang (Eds)

MECHANICAL MODEL OF ADHESIVE POST-INSTALLED ANCHOR SUBJECTED TO CYCLIC SHEAR FORCE

**YUYA TAKASE*, TOSHINAGA WADA†, TAKAAKI IKEDA††
AND YASUJI SHINOHARA†††**

* Research Inst. of Technology, Tobishima Corporation,
Noda-shi, Chiba, JAPAN
e-mail: yuya_takase@tobishima.co.jp, web page: http://www.tobi-tech.com

† Department of Architechture, Hokkaido Polytechnic College,
Otaru-shi, Hokkaido, JAPAN
e-mail: wada@hokkaido-pc.ac.jp, web page: http://www3.jeed.or.jp/hokkaido/college/

†† Research Inst. of Technology, Tobishima Corporation,
Noda-shi, Chiba, JAPAN
e-mail: takaaki_ikeda@tobishima.co.jp, web page: http://www.tobi-tech.com

††† Structure Eng. Research Center, Tokyo Institute of Technology,
Yokohama-shi, Kanagawa, JAPAN
e-mail: shinohara.y.ab@m.titech.ac.jp, web page: http://www.serc.titech.ac.jp/

Key words: Post-installed Anchor, Dowel Action, Adhesive Anchor, Seismic Retrofitting

Abstract: Recently, it has become increasingly important to instigate more widespread seismic retrofitting for seismically weak structures in Japan, which is frequently subject to massive earthquakes. Generally, post-installed anchors are used to connect the seismic retrofitting members to existing members. However, no computational models of post-installed anchors have yet been proposed in previous studies to evaluate stress-displacement relationships. Accordingly, we developed a new mechanical model for post-installed anchors. In this model, the kinking behavior of anchor bolts, bearing behavior of concrete, and tensile behavior of anchor bolts are considered. The proposed model can reasonably simulate the mechanical behaviors of the previous test results.

1 INTRODUCTION

Recently, it has become increasingly important to instigate more widespread seismic retrofitting systems for seismically weak structures in Japan, since not only is it one of the most seismically active countries in the world, but many of these earthquakes are very severe.

Generally, post-installed anchors are used to connect the seismic retrofitting members to existing members. Post-installed anchors are used for significant elements in reinforced concrete structures, because shear stress is transferred through post-installed anchors during earthquakes. Accordingly, it is necessary to evaluate this shear stress transfer mechanism from a theoretical perspective for safe structural designs when undertaking seismic retrofitting.

The dowel action of reinforcement bars has been previously investigated by many researchers[1]-[3], but no computational model of post-installed anchors has ever been proposed to estimate the stress-displacement relationship.

Therefore, we developed a new mechanical model for post-installed anchors. In this model, the kinking force of anchor bolts, bearing stress of concrete, and tensile stress of anchor bolts

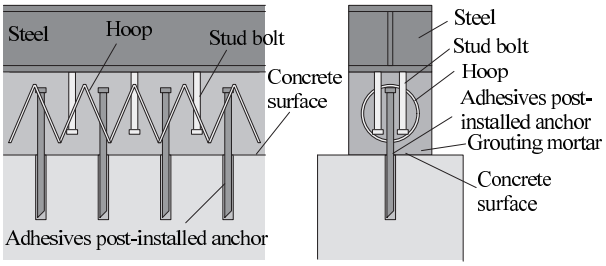

Figure 1: An example of a join for seismic retrofitting

are considered. The mechanical behaviors of these components are formulated respectively.

In this paper, details of the proposed model and their adequacy in terms of test results are described.

2 PROPOSED MODEL

We constructed a dowel model of a adhesive post-installed anchor subjected to shear loading using the piles theory based on the elastic beam theory. The failure modes of the post-installed anchors in this paper are: i) yield of anchor bolt, and ii) bearing failure of concrete.

2.1 Equilibrium of Shear Force

Figure 1 shows an example of the joint for seismic retrofitting. Figure 2 presents an image of dowel action modeling for a post-installed anchor. When the displacement is small, it is possible to apply the elastic beam theory to a post-installed anchor.

$$E_S I_Z \frac{d^4 \delta_a}{dx^4} + \phi\kappa(x, \delta_a) = 0 \tag{1}$$

Here, E_s is the Young's modulus of an anchor bolt, I_z is the second moment of area, δ_a is the displacement of an anchor bolt, and ϕ is the diameter of an anchor bolt.

However, when an anchor bolt or concrete are within their plastic range, the elastic beam theory should not be applied. Therefore, we proposed the model as shown in Figure 2 to better describe the behavior in a nonlinear zone. In the proposed model, initially the plastic hinge is calculated.

Assuming the anchor bolt deforms in a linear manner around the plastic hinge, the bearing stress acts on the concrete. Furthermore, the anchor bolt elongates between the concrete surface and the plastic hinge. Thus, the anchor bolt is subject to tensile stress, which is the shear component of this stress. As above, the shear force equates to: i) the bending moment of the plastic hinge, ii) the bearing stress of the concrete, and iii) a shear component of the tensile stress of the anchor bolt as shown in Figure 3.

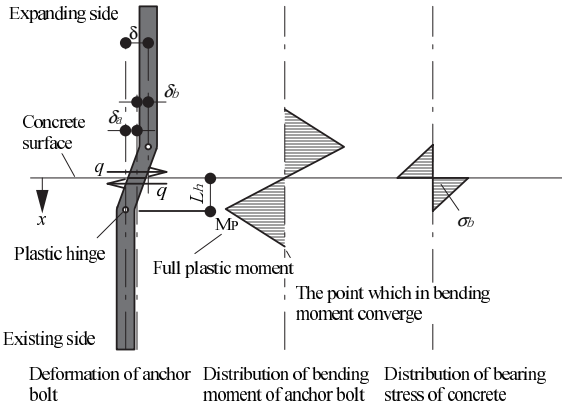

Figure 2: Modeling of dowel action for a post-installed anchor

$$q = q_S + q_B + q_T^S \tag{2}$$

2.1 Depth of Plastic Hinge

The depth of the plastic hinge influences the three components of the shear force. According to the elastic beam theory, the largest moment depth L_M is derived from the following equation.

$$L_M = \frac{\pi}{4}\sqrt[4]{\frac{4E_s I_Z}{\kappa\phi}} \tag{3}$$

Here, κ is the reaction modulus of the concrete.

But, when concrete is in its plastic range, κ becomes smaller. Conversely, L_M gets larger. Figure 2 shows the relationship between increasing the ratio of depth and reducing the ratio of the reaction modulus of concrete. The increase ratio will be 2 if the reduction ratio of the reaction modulus is reduced to 1/20. As a result, the depth of the plastic hinge point L_h is obtained in this paper.

$$L_h = \frac{3\pi}{8}\sqrt[4]{\frac{4E_s I_Z}{\kappa\phi}} \tag{4}$$

Maekawa's model[4] is used in this model for the reaction modulus of concrete.

$$\kappa = 150\sigma_B/\phi \tag{5}$$

Here, σ_B is the concrete compressive stress (N/mm^2). From Eqs. (4) and (5), a shear force yielding anchor bolt is obtained as follows.

$$q_P = M_P / L_h \tag{6}$$

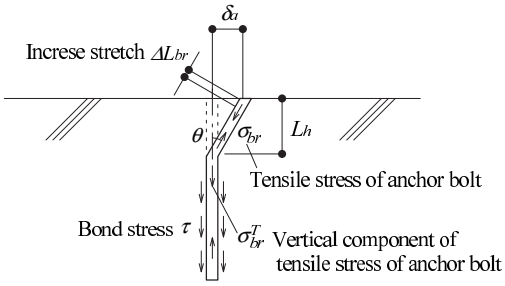

Figure 3: Tensile Stress of Anchor Bolt

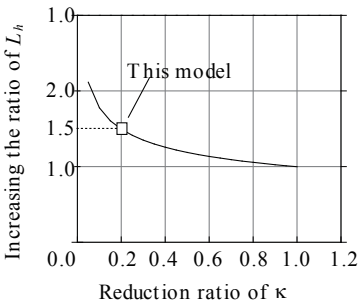

Figure 4: Relationship between ΔL_h and $\Delta\kappa$

The plastic moment is as follows.

$$M_P = \frac{\phi^3 \cdot \sigma_y}{6} \tag{7}$$

Here, σ_y is the yield stress of the anchor bolt (N/mm^2). The bending resistance force is influenced by q_p. The bending resistance behavior is mentioned in Section 2.5.

2.3 Bearing Stress of Concrete

The concrete strain is influenced by the deformation of an anchor bolt. Assuming that the anchor bolt deforms linearly around the plastic hinge, the slip of anchor bolt δ_a is described as follows.

$$\delta_a(x) = \begin{cases} \delta_a(0) - \dfrac{\delta_a(0)}{L_h} \cdot x & (0 \le x < L_h) \\ 0 & (L_h \le x) \end{cases} \tag{8}$$

It is thought that concrete strain is greater near the anchor bolt, and less further away. However, it is difficult to review this phenomenon. Therefore, the concrete strain is described as the average strain.

$$\varepsilon_b(x) = \delta_a(x)/L_{\varepsilon b} \tag{9}$$

Here, $L_{\varepsilon b}$ is the effective length leading to concrete strain.

The bearing force of the concrete is calculated by multiplying the circumference of the semicircle of the anchor bolt and integration from $x = 0$ to $x = L_h$.

$$q_B = \frac{\pi\phi}{2}\int_0^{L_h} \sigma_b(x)dx \tag{10}$$

2.4 Tensile Stress of Anchor Bolt

When the anchor bolt deforms around the plastic hinge, the anchor bolt is stretched between the plastic hinge and the concrete surface. The increase in length ΔL_{br} is as follows.

$$\Delta L_{br} = \sqrt{\Delta\delta_a^2 + L_h^2} - L_h \tag{11}$$

The strain ε_{br} is obtained from ΔL_{br}. Moreover, its shear component force $q_T{}^S$ is expressed as follows.

$$\Delta\varepsilon_{br} = \Delta L_{br}/L_h \tag{12}$$

$$q_T^S = q_T \sin\theta = \sigma_{br}\frac{\pi\phi^2}{4}\sin\theta \tag{13}$$

In addition, because the adhesion bond is hardly damaged between the plastic hinge and the concrete surface, it is thought that the bond between these is not affected .

2.5 Mechanical Behavior of Three Components

Figure 5 shows the mechanical behaviors. In this section, the mechanical behaviors are explained.

(1) Bending Resistance of Plastic Hinge

In this model, the behavior of the bending resistance of the plastic hinge is considered to be the same as the behavior of the reinforcement bar subjected to tensile stress. As a constitutive equation, the Menegotto-Pinto model[5] is used here. Fine tuning this model, the behavior of the bending resistance of the plastic hinge is expressed as follows.

$$\tilde{q}_S = R_s\tilde{\delta}_a + \frac{(1-R_s)\tilde{\delta}_a}{\left(1+\tilde{\delta}_a^{R_b}\right)^{1/R_b}} \tag{14a}$$

$$\tilde{\delta}_a = \frac{\delta_a - \delta_r}{\delta_0 - \delta_r} \tag{14b}$$

$$\tilde{q}_S = \frac{q_S - q_r}{q_0 - q_r} \tag{14c}$$

$$R_s = \frac{K_{s2}}{K_s} \tag{14d}$$

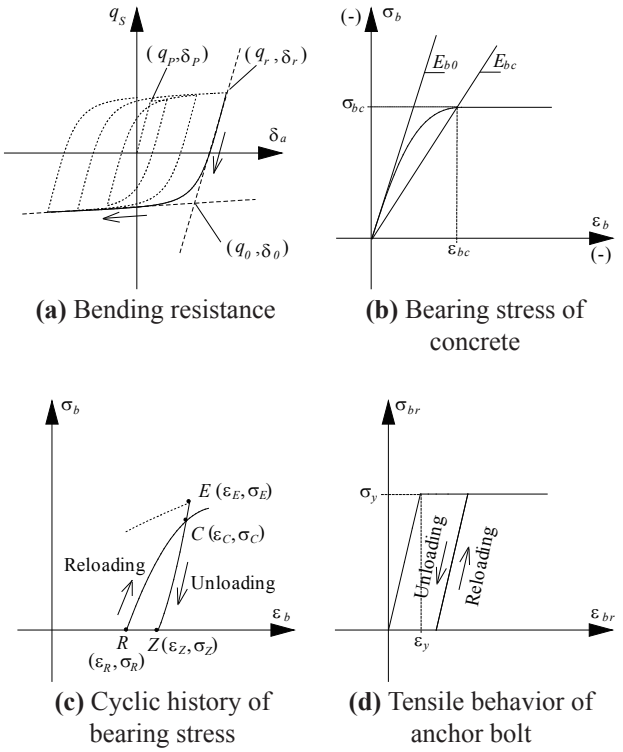

(a) Bending resistance **(b)** Bearing stress of concrete

(c) Cyclic history of bearing stress **(d)** Tensile behavior of anchor bolt

Figure 5: Mechanical behaviors

$$q_0 = K_S(\delta_0 - \delta_r) + q_r \tag{14e}$$

$$\delta_0 = \begin{cases} \dfrac{q_P - q_r + E_s(\delta_r - R_s\delta_p)}{K_s(1-R_s)} & \dot{\delta}_s \geq 0 \\ \dfrac{-q_P - q_r + E_s(\delta_r + R_s\delta_p)}{K_s(1-R_s)} & \dot{\delta}_s < 0 \end{cases} \tag{14f}$$

R_b is the parameter expressing the Bauschinger effect as follows.

$$R_b = R_{b0} - \frac{a_1\xi}{a_2+\xi} \tag{15a}$$

$$\xi = \frac{|\delta_0 - \delta_r'|}{\delta_p} \tag{15b}$$

In these equations, R_{b0}, a_1 and a_2 are material coefficients. Here, R_{b0} is 20, a_1 is 18.5 and a_2 is 0.15 based on a general coefficient for reinforcement bars.

(2) Bearing Stress of Concrete

The bearing stress is regarded as the local compressive stress. Therefore, the constitutive equation of the compressive stress[6] are applied to the bearing stress of concrete up to the maximum stress.

$$\sigma_b = \frac{E_{b0}\cdot\varepsilon_b}{1+\left(\dfrac{E_{b0}}{E_{bc}}-2\right)\left(\dfrac{\varepsilon_b}{\varepsilon_{bc}}\right)+\left(\dfrac{\varepsilon_b}{\varepsilon_{bc}}\right)^2} \tag{16}$$

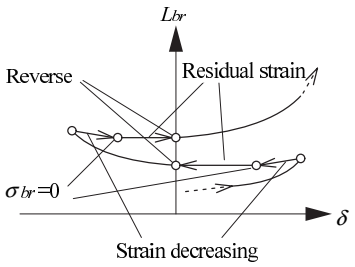

Figure 6: Behavior of anchor bolt

After the maximum stress, the stress remains elevated because the anchor bolt is restrained. Moreover, the maximum bearing stress exceeds the maximum compressive stress. In this model, the following equation is proposed for the maximum bearing stress.

$$\sigma_{bc} = 2.5\cdot\sigma_B^{0.8} \tag{17}$$

The behavior of the bearing stress under cyclic loading is expressed as follows.

$$\sigma_b = a\varepsilon_b^2 + b\varepsilon_b + c \tag{18a}$$

$$E_E = 1.5E_{EZ} \quad \left(E_E \leq \frac{2\sigma_E}{\varepsilon_E - \varepsilon_Z}\right) \tag{18b}$$

$$\varepsilon_Z = \varepsilon_E - 0.05\cdot\varepsilon_P \tag{18c}$$

$$\varepsilon_R = \left[0.145\left(\frac{\varepsilon_E}{\varepsilon_P}\right)^2 + 0.127\left(\frac{\varepsilon_E}{\varepsilon_P}\right)\right]\varepsilon_P \tag{18d}$$

$$\varepsilon_R = \left[\frac{\varepsilon_E}{\varepsilon_P} - 2.828\right]\varepsilon_P \quad \left(|\varepsilon_E| \geq 4.0|\varepsilon_P|\right) \tag{18e}$$

These equations are based on the previous studies[8],[9].

(3) Tensile Stress of Anchor Bolt

The behavior of the tensile stress is applied to a bilinear model as in Figure 5 (d). Moreover, the behavior of L_{br} subjected to cyclic loading is presented in Figure 6.

3 ADAPTABILITY OF PROPOSED MODEL TO TEST RESULTS

3.1 Test Parameters

Table 1 shows the test parameters for using this verification. Figure 7 shows the image of the loading of these test[10]~[13].

Table 1: Summary of the specimens parameters

No.	Loading History	ϕ (mm)	σ_B (N/mm^2)	σ_G (N/mm^2)	Type
M-1[10]	Mono.	19	24.7	-	Capsule
M-2[10]	Mono.	19	14.7	-	Capsule
M-3[10]	Mono.	16	14.7	-	Capsule
M-4[11]	Mono.	19	30.4	-	Injection
C-1[12]	Cyc.	13	31.3	55.4	Injection
C-2[13]	Cyc.	16	14.7	28.7	Injection

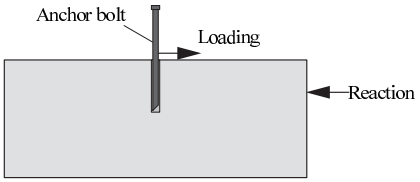

(a) Specimens M-1 ~ M-4

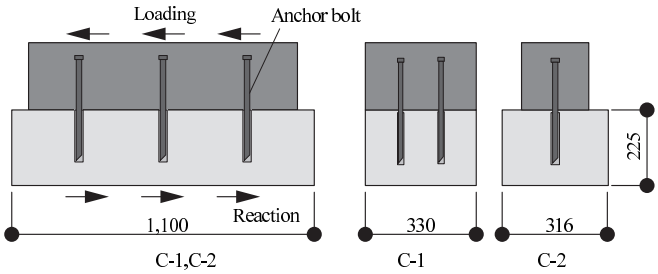

(a) Specimens C-1 and C-2

Figure 7: Image of the loading

In this paper, only test specimens used in organic adhesives are considered. Two loading histories are applied, i.e. monotonic loading and cyclic loading.

The test parameters for comparison are the concrete compressive strength σ_B and the diameter of the anchor bolt ϕ. The values of σ_B are in the range 14.7 to 31.3 N/mm^2, whereas ϕ is either 16 mm or 19 mm.

The specimen name is derived from the code indicated by the loading history (M or C) and a serial number.

The anchor bolts are made from normal strength f_y = 295 N/mm^2 or f_y = 345 N/mm^2, except for specimen C-2, which alone was made of high-strength SNB-7(σ_y = 821 N/mm^2) material.

Adhesive anchors are classified as capsule type or injection type. Specimens M-1, M-2, M-3 are capsule types, and specimens M-4, C-1, C-2 are injection types.

3.2 Monotonic Loading

Figure 8 shows a comparison of the test and analysis results from the M-1 to M-4 specimens.

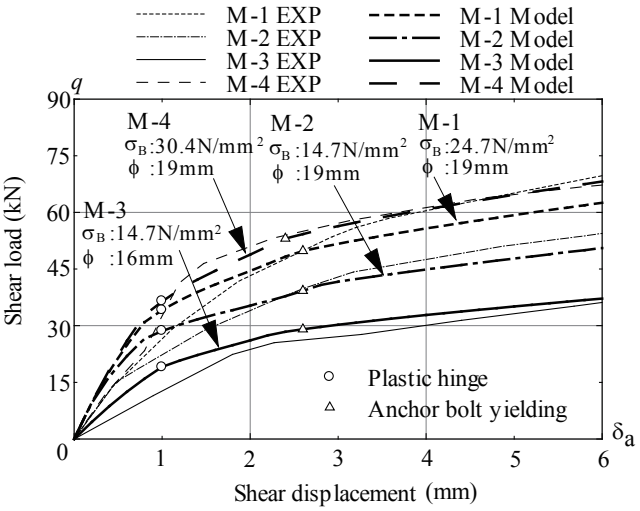

Figure 8: Specimens M-1 ~ M-4

Initially, the M-1 and M-2 specimens were compared. These specimens are made of the same material, f_y = 345 N/mm^2, and have the same diameter, ϕ = 19 mm, but are used in concretes with different compressive strengths: σ_B = 24.7 and σ_B = 14.7 N/mm^2. These test curves demonstrate the same behavior almost until δ_a = 2 mm. But the reduced stiffness of the M-2 specimen is gradually more noteable after δ_a = 2 mm. Overall, the analysis curves are well evaluated, although a bit large until δ_a = 2 mm.

Secondly, the M-2 and M-3 specimens were compared. These specimens differ only in the diameter of the anchor bolt. Overall, the analysis results are well evaluated against the test results, although the initial stiffness of the analysis was a bit high.

Injection-type adhesive anchors are only used in the M-4 specimen. The test behavior was evaluated by analysis. As a result, it seems that the difference in adhesive type has less effect.

3.2 Cyclic Loading

Figures 9 and 10 show a comparison of the test results and analysis results for specimens C-1 and C-2 respectively.

Actually, it is necessary to consider deformation of the joint side. In this paper, it is presupposed that the joint side deforms as a rigid body.

The initial stiffness of the analysis exceeds the test results until δ_a is about 2 mm in Figure 9. But the analysis and test results demonstrate correspondence above δ_a = 2 mm. Based on these tendencies, it appears that the adherence

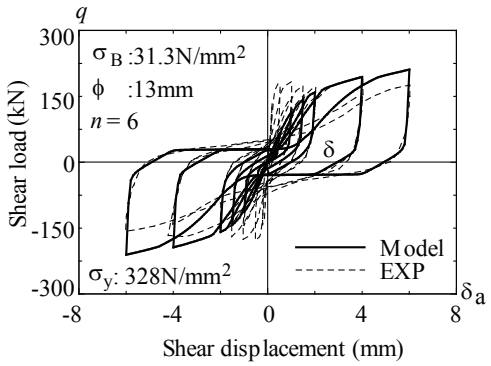

Figure 9: Spesimen C-1

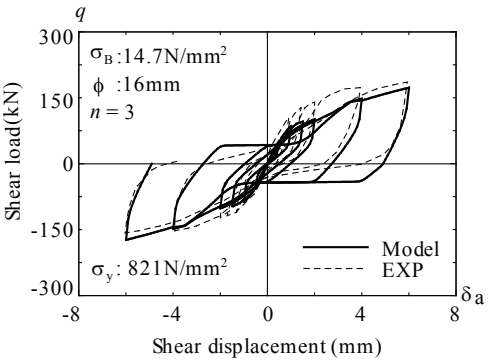

Figure 10: Spesimen C-2

strength of the concrete surface may be affected. In this model, the adherence strength of the concrete surface is not considered. Therefore, the initial stiffness of the analysis is less until the adherence effect is overcome. However, the behavior after the adherence no longer has an effect, in unloading and in reloading, are accurately evaluated overall in this analysis.

Next, Figure 10 is observed. On the positive loading, the initial stiffness of the analysis is excessive in the same manner as the C-1 specimen. But on the negative loading, the initial stiffness of the analysis replicates the test. It is thought that the adherence effect is less because of the low compressive strength of grouting mortar. However, the overall behavior of the test result is estimated by the proposed model.

Based on the observations in this section, the proposed model is able to evaluate test results reasonably for engineering purposes.

4 CONCLUSIONS

We proposed a dowel model of a post-installed anchor subjected to shear force. In this model, the shear force equates to the sum of the bending resistant force q_s, the bearing stress of concrete q_B, and the shear component of the tensile stress q_T^S. Findings obtained in this paper are as follows:

1) The proposed model could estimate the q-δ curves of post-install anchors subjected to monotonic shear force.
2) The experimental results were estimated by analysis ignoring deformation of the joint side.
3) Unloading and reloading behaviors can be estimated using the proposed model.

We will strive for a modification to simulate the behavior when subjected to both shear and tensile forces with due consideration for the bonded stress – slip behavior of the adhesive anchor bolts.

ACKNOWLEDGMENT

This work was supported by JSPS KAKENHI Grant Number 23760542.

REFERENCES

[1] Hofbeck, J. A., Ibrahim, I. O. and Mattock, A. H., 1969, Shear transfer in reinforced concrete, J. of ACI, No.66; pp.119-128.

[2] Jimenez, R., White, R. N. and Gergely, P., 1982, Cyclic shear and dowel action models in R/C, J. of ASCE, Vol.108, No.ST5; pp.1106-1123.

[3] Vintzeleou, E. N.and Tassios, T. P., 1986, Mathematical models for dowel action under monotonic and cyclic conditions, Magazine of concrete research, Vol.38, No.134; pp.13~22.

[4] Maekawa, K. and Qureshi, J., 1996, Ccomputational model for reinforcing bar embedded in concrete under combined axial pullout and transverse displacement, J. materials, Conc. Struct., Pavements., JSCE; pp.227-239. (in English)

[5] Menegotto, M. and Pinto, P. E., 1973, Method of analysis for cyclically loaded R.C. plane frame including changes in geometory and non-elastic behavior of elements under combined normal force and bending, Pfoc. of IABSE, Symposiium on Resistance and Ultimate Deformability of

Structures Acted on by Well Defined Repeated Loads; pp.15-22.

[6] Saenz, L. P., 1983, Discussion of Equation for Stress - Strain Curve of Concrete, by Desayi P. and Krishnan S., ACI Journal, V. 61, No. 9; pp.1227-1239.

[7] Ollgaard, J. G., Slutter, R. G. and Fisher, J. W., 1971, Shear strength of stud connectors in lightweight and normal-weight concrete, AISC Eng. Journal; pp.55-64.

[8] Karsan, I. D. and Jirsa, J. O., 1969, Behavior of Concrete under Compressive Loading, Journal of ASCE, Vol.95, No. ST2; pp.2543-2563.

[9] Naganuma, K. and Ohkubo, M., 2000, An analytical model for reinforced concrete panels under cyclic stresses, Journal of strutural engneering, AIJ, No.536; pp.135-142.

[10] Fukumoto,K., Kiyohara, T., Nakano, K. and Matsuzaki, Y., 1998, Experimental study on structural performance of post installed bonded anchors, Summaries of technical papers of Annual Meeting, AIJ, C-2; pp.719-720.(in Japanese)

[11] Ando, Y. and Nakano, K., 2008, Influence of edge distance for shear capacity of post-installed bonded anchor, Proceedings of annual research meeting Hokuriku Chapte, AIJ, No.51; pp.77-80.(in Japanese)

[12] Tsuyoshi, M., Sadasue, K., Ishimura, M. and Minami, K., 2010, Experimental study on post-installed diagonal anchor, Proceedings of the Japan Concrete Institute, Vol.32, No.2; pp.985-990.(in Japanese)

[13] Sadasue, K., Hosokawa, Y., Oka, K. and Minami, K., 2009, Experimantal study of shear strength of disk anchor, Proceedings of the Japan Concrete Institute, Vol.31, No.2; pp.1009-1014.(in Japanese)